

Design of Flow Channel with Surface Electrodes to Detect Dielectrophoretic Movement of Floating Myoblast

Shigehiro HASHIMOTO, Daisuke HASEGAWA, Yusuke TAKAHASHI, Ryota MATSUZAWA

Biomedical Engineering, Department of Mechanical Engineering,
Kogakuin University, Tokyo, 163-8677, Japan
<http://www.mech.kogakuin.ac.jp/labs/bio/>

ABSTRACT

A micro flow channel with the surface electrodes has been designed to detect the dielectrophoretic movement of a biological cell *in vitro*. A pair of asymmetric surface electrodes of titanium (thickness of 200 nm) were incorporated in the flow channel by the photolithography technique: a triangular electrode with the tip angle of 0.35 rad, and a rectangular electrode of the flat edge as reference. The rectangular cyclic alternating electric current was introduced between the surface electrodes. The suspension of C2C12 (mouse myoblast cell line) was injected into the flow channel, and the flow rate was controlled by the pressure head between the inlet and the outlet. The selected system design (the shape of the electrode, electric rectangular alternating current wave (± 7.5 mA, $0.3 \mu\text{s}$ of period), and the flow velocity of 0.3 mm/s) is able to detect dielectrophoretic movement of floating C2C12.

Keywords: Biomedical Engineering, Dielectrophoresis, Surface Electrode and C2C12.

1. INTRODUCTION

The movement of a biological cell suspended in the medium is governed by several factors: electric force, Van der Waals force, affinity of surface, and pressure. Various methods have been applied to control the movement of cells *in vitro*: the flow [1], slits [2, 3], the magnetic field [4], the gravitational field [5, 6], and the electric field [7]. These methods might contribute to several applications of manipulation of cells: arrangement of cells to make a tissue, sorting of cells, and measurement of the character of cells.

Movement of a charged particle depends on the electric field. The effect is applied to the electrophoresis device. When a particle is subjected to a non-uniform electric field, a force acts even on a non-charged particle, because the polarization generates in the particle. The phenomenon is called dielectrophoresis [8–26], which depends on the several parameters: the electrical property of the particle, shape and size of the particle [8], the electrical property of the medium, and frequency of the electric field. Electrophoresis is a phenomenon, in which a particle is moved by the Coulomb force between the charge of the particle and the electric field. Dielectrophoresis [9], on the other hand, is a phenomenon, in which a particle moves due to the interaction between the electric field and the charge induced in a neutral particle, when the particle is placed in a non-uniform electric field. The force

of dielectrophoresis is calculated by the equivalent dipole moment method.

$$F = \pi \varepsilon_m r^3 \text{Re} [K(\omega)] \nabla E^2 \quad (1)$$

In Eq. 1, r is the radius of the particle, ε_m is the dielectric constant of the surrounding medium, and E is the maximum value of the electric field. $\text{Re} [K(\omega)]$ represents the real part of the function expressed by the following equation.

$$K(\omega) = (\varepsilon_p^* - \varepsilon_m^*) / (\varepsilon_p^* + 2 \varepsilon_m^*) \quad (2)$$

In Eq. 2, ε_p^* is the complex dielectric constant of the particle, ε_m^* is the complex dielectric constant of the solution.

With the aid of the micromachining technique [27], many kinds of micro systems were designed, in which dielectrophoresis was applied to sorting of biological cells floating in the medium in the previous studies. In the present study, a micro flow channel with the surface electrodes has been designed to detect the dielectrophoretic movement of a biological cell *in vitro*.

2. METHODS

Surface Electrode

The titanium film was used for the surface electrode. Titanium was coated on the glass plate ($36 \text{ mm} \times 28 \text{ mm} \times 1 \text{ mm}$, Matsunami Glass Ind., Ltd., Japan). The thickness of coating is 200 nm. The tip angle of the triangle shape of the one of the surface electrodes is 0.35 rad. The other reference electrode has a flat edge. The distance between electrodes is 0.1 mm (Fig. 1). The shortest connecting line between electrodes is vertical to the flow direction.

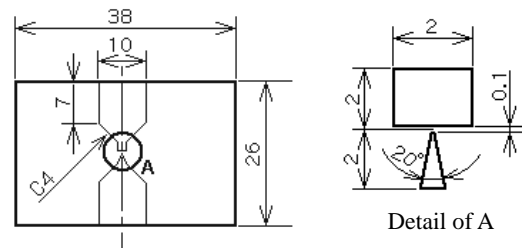


Fig. 1: Dimension of surface electrode: unit mm.

Deposition of Titanium

Before the deposition of titanium, the surface of the glass plate was hydrophilized by the oxygen ($30 \text{ cm}^3/\text{min}$, 0.1 Pa) plasma ashing for five minutes at 200 W (20 Pa) by the reactive ion etching system (FA-1, Samco International, Kyoto, Japan). Titanium was deposited on the surface of the glass plate with 200 nm thickness in the electron beam vapor deposition apparatus (JBS-Z0501EVC JEOL Ltd., Tokyo, Japan).

Photomask A for Triangle Tip of Electrode

Before the deposition of titanium, the surface of the plate was hydrophilized by the oxygen ($30 \text{ cm}^3/\text{min}$, 0.1 Pa) plasma ashing for five minutes at 200 W (20 Pa) by the reactive ion etching system (FA-1). The positive photoresist material of OFPR-800LB-20cP (Tokyo Ohka Kogyo Co., Ltd, Tokyo, Japan) was coated on the titanium with the spin coater (at 3000 rpm for 30 s). The photoresist was baked at the hotplate at 338 K for one minute and at 368 K for three minutes, successively.

The pattern of the electrode with the flow channel was drawn on the mask with a laser drawing system (DDB-201K-KH, Neoark Corporation, Hachioji, Japan). The photoresist was developed with tetra-methyl-ammonium hydroxide (NMD-3, Tokyo Ohka Kogyo Co., Ltd., Kawasaki, Japan) for two minutes, rinsed with the distilled water, and dried.

The titanium coated plate was etched with the plasma gas using RIE-10NR (Samco International, Kyoto, Japan). For etching, the gas of SF_6 ($50 \text{ cm}^3/\text{min}$ at 1013 hPa) with Ar ($50 \text{ cm}^3/\text{min}$ at 1013 hPa) was applied at 75 W at 4 Pa for seven minutes.

Photomask B for Electrode

The titanium coated glass plate was hydrophilized by the oxygen ($30 \text{ cm}^3/\text{min}$, 0.1 Pa) plasma ashing for five minutes at 100 W by the reactive ion etching system (FA-1). The negative photoresist material of low viscosity (SU-8 2: Micro Chem Corp., MA, USA) was coated on the titanium with the spin coater (at 3000 rpm for 30 s) (Fig. 2). The photoresist was baked at the hotplate at 338 K for one minute and at 368 K for three minutes, successively.

The photomask A was mounted on the surface of SU-8, and the photoresist was exposed to the UV light through the mask in the mask aligner (M-1S, Mikasa Co. Ltd., Japan) for 15 s . The photoresist was baked at the hotplate at 338 K for one minute and at 368 K for three minutes, successively. The photoresist was developed with SU-8 Developer (Micro Chem Corp., MA, USA) for two minutes. The glass surface with the micro pattern was rinsed with IPA (2-propanol, Wako Pure Chemical Industries, Ltd.) for one minute, and with pure water for one minute. After drying, the plate was etched with the plasma gas using RIE-10NR. For etching, the gas of SF_6 ($50 \text{ cm}^3/\text{min}$ at 1013 hPa) with Ar ($50 \text{ cm}^3/\text{min}$ at 1013 hPa) was applied at 75 W at 4 Pa for seven minutes. The areas at the bands of both ends were covered with the polyimide tapes (protect photoresist material from ultraviolet light) to leave the part of titanium coating for extended electrodes.

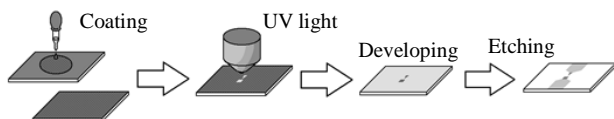


Fig. 2: Photolithography process for photomask B.

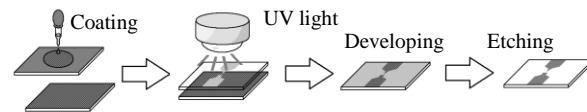


Fig. 3: Photolithography process for surface electrodes.

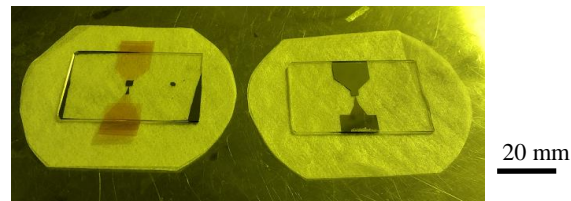


Fig. 4: Photomask B (left), and surface electrodes (right).

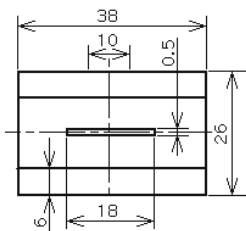


Fig. 5: Dimension of photomask C for flow channel: unit mm.

Surface Electrodes

The titanium coated glass plate was hydrophilized by the oxygen ($30 \text{ cm}^3/\text{min}$, 0.1 Pa) plasma ashing for five minutes at 100 W by the reactive ion etching system (FA-1). The positive photoresist material of OFPR-800LB-20cP was coated on the titanium with the spin coater (at 3000 rpm for 30 s) (Figs. 3&4). The photoresist was baked at the hotplate at 338 K for one minute and at 368 K for three minutes, successively. The photomask B was mounted on the surface of SU-8, and the photoresist was exposed to the UV light through the mask in the mask aligner (M-1S) for 15 s . The photoresist was developed with tetra-methyl-ammonium hydroxide (NMD-3) for two minutes, rinsed with the distilled water. After drying, the plate was etched with the plasma gas using RIE-10NR. For etching, the gas of SF_6 ($50 \text{ cm}^3/\text{min}$ at 1013 hPa) with Ar ($50 \text{ cm}^3/\text{min}$ at 1013 hPa) was applied at 75 W at 4 Pa for seven minutes.

Lower Plate of Flow Channel

To make the groove of the flow channel (width of 0.5 mm , length of 18 mm , and depth of 0.04 mm), the photomask C (Fig. 5) was made by the same process as the photomask A. The surface of the electrodes was hydrophilized by the oxygen ($30 \text{ cm}^3/\text{min}$, 0.1 Pa) plasma ashing for five minutes at 200 W (20 Pa) by the reactive ion etching system (FA-1). The negative photoresist material of low viscosity (SU-8 100) was coated on the surface electrodes with the spin coater (at 1300 rpm for 30 s , and at 2700 rpm for 120 s , successively) (Fig. 6). The coating condition was adjusted to make the layer of thickness (correspond to the height of the flow channel) between $20 \mu\text{m}$ and $40 \mu\text{m}$. The thickness of the layer (SU-8 100) on the surface electrode was measured by the stylus (with $3 \times 10^{-5} \text{ N}$) of the contact profilometer (Dektak XT-E, Bruker Corporation). (Fig. 10) The photoresist was baked at the hotplate at 338 K for ten minutes and at 368 K for seventy minutes, successively.

The photomask C was mounted on the surface of SU-8, and the photoresist was exposed to the UV light through the mask in the

mask aligner (M-1S) for 20 s. The photoresist was baked at the hotplate at 338 K for seven minutes and at 368 K for fifteen minutes, successively. The photoresist was developed with SU-8 Developer for eight minutes. The surface with the micro pattern was rinsed with IPA, and with pure water. The photoresist was baked at the hotplate at 368 K for twenty minutes.

Upper Plate of Flow Channel

PDMS was poured into the mold of poly-methyl-methacrylate (Fig. 7) with the curing agent. The volume ratio of PDMS to curing agent is ten to one. After degassing, PDMS was baked at 353 K for two hours in the oven (DX401, Yamato Scientific Co., Ltd). The upper plate has holes with the diameter of 5 mm for the inlet and the outlet of the suspension.

Flow Channel

The upper plate was exposed to the oxygen gas (0.1 Pa, 30 cm³/min) in the reactive ion etching system (FA-1) (50 W, 20 Pa, for two hours). Aminopropyltriethoxysilane (APTES) was coated on the upper plate. After ten minutes, the upper plate was adhered on the lower plate under the pressure of 0.5 N/m² by sandwiching between plates of poly-methyl-methacrylate. The value of the pressure was selected between 0.25 N/m² and 0.8 N/m² to control the height of the flow channel between plates. The plates were baked in the oven at 353 K for ten minutes. A rectangular parallelepiped channel of 18 mm length \times 0.5 mm width \times 0.035 mm height is formed between upper and lower plates (Fig. 7). The flow channel is placed on the stage of the inverted phase-contrast microscope (IX71, Olympus Co., Ltd., Tokyo) (Fig. 7).

Electric Stimulation

The electric stimulation (E) of the alternating rectangular cyclic wave ($0.3 \mu\text{s} < \text{period} < 10 \mu\text{s}$; $\pm 5 \text{ V}$, $\pm 10 \text{ V}$, or $\pm 15 \text{ V}$) was generated with an electric stimulator. The stimulator was connected to the titanium film electrode, and the electric stimulation was applied to the medium of cells. An electric resistance (R) of 2 k Ω is serially inserted between the electrode and the stimulator (Fig. 8). The electric signal between the terminals of the resistance (V) is monitored by an oscilloscope during electric stimulation applied between the titanium surface electrodes (Fig. 11b).

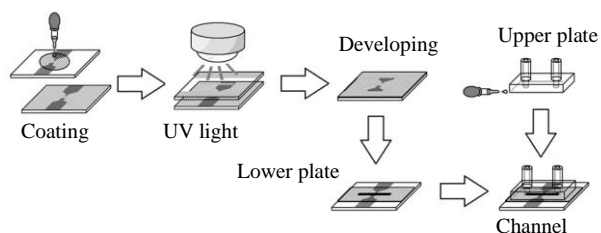


Fig. 6: Photolithography process for flow channel.

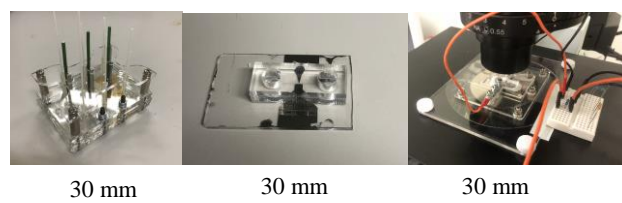


Fig. 7: Mold for upper plate of flow channel (left), upper plate of flow channel on lower plate with electrodes (middle), flow channel on stage of microscope (right).

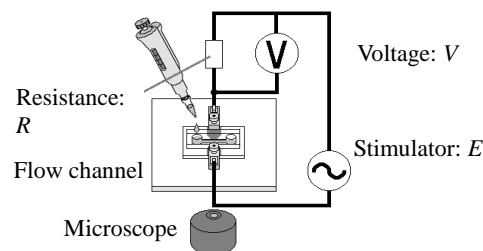


Fig. 8: Flow channel with electric circuit.

Cell

C2C12 (mouse myoblast cell line originated with cross-striated muscle of C3H mouse) was used in the test. D-MEM (Dulbecco's Modified Eagle Medium) containing 10% FBS (Fetal Bovine Serum) and 1% penicillin/ streptomycin was used for the medium.

Before the flow test, the inner surface of the flow channel was hydrophilized by the oxygen (30 cm³/min, 0.1 Pa) plasma ashing for two minutes at 50 W by the reactive ion etching system (FA-1). The bovine serum albumin solution was pre-filled in the flow channel, and incubated for thirty minutes at 310 K in the incubator.

Before the flow test, the cells were exfoliated from the plate of the culture dish with trypsin including EDTA (ethylenediaminetetraacetic acid), and suspended in the medium. The suspension of cells was poured at the inlet of the flow channel. The flow occurs by the pressure difference between the inlet and the outlet, which was kept by the gravitational level of the medium ($< 5 \text{ mm}$).

Each cell passing between the electrodes was observed by the inverted phase-contrast microscope (IX71), and recorded by the camera (DSC-RX100M4, Sony Corporation, Japan), which is set at the eyepiece of the microscope. The movement of the cell was analyzed by "Kinovea (Ver. 8.23, Commons Attribution)" at the video images: 30 frames per second. To trace the movement of the cell, the coordinates are defined as that in Fig. 9. The flow direction is defined as x . The perpendicular direction from the reference electrode to the tip of the triangular electrode is defined as y . The origin is adjusted at the tip of the triangular electrode. Both the position (x_0 , y_0) and the velocity (v_0) of each cell were measured at $x = -0.4 \text{ mm}$ (upstream from the tip of the electrode) as the initial value. The shifted distance (Δy) was defined as the difference between the maximum value of y coordinate and minimum value of y coordinate according to the stream line of each cell.

3. RESULTS

Fig. 10 shows the tracings of the stylus on the layer of SU-8 on the surface electrode. The tracings show that the thickness of layer of SU-8 is 34 μm .

Fig. 11 exemplifies tracings of the voltage of electric stimulation of rectangular cyclic waves: the voltage between terminals of the electric stimulator (E in Fig. 11a), and the voltage between terminals of the resistance of 2 k Ω (V in Fig. 11b). The tracings show the following values: the period of 1 μs , and the amplitude of $\pm 15 \text{ V}$. The electric current is

calculated from the electric voltage divided by the electric resistance (2 kΩ). Fig. 11b shows the rectangular alternating electric current (± 7.5 mA) flows the electric circuit.

In Fig. 12, each colored line shows the movement of each cell in the stationary fluid around the triangle electrode with electric stimulation (rectangular wave, period of 1 μ s, amplitude of ± 15 V). Every cell near the lower plate moves to the triangle electrode by dielectrophoresis.

Fig. 13 shows cells in flow channel around the triangular electrode. Every cell passing near the tip of the electrode changes the flow direction near the electrode.

Fig. 14 shows the shifted distance (Δy) in relation to the amplitude of the rectangular alternating voltage (E). The mark shows the mean value of Δy , and the bar shows the standard deviation. The shifted distance increases with the increase of the amplitude of the voltage. Fig. 15 shows the relationship between the shifted distance (Δy) and the initial velocity (v_0) of the cell. The shift decreases with the initial velocity. Fig. 16 shows the relationship between the shifted distance (Δy) and the period (T [μ s]) of cyclic rectangular alternating electric stimulation. The shift decreases with the period of cyclic stimulation.

Fig. 17a shows the relationship between the shifted distance (Δy) and the dimension of cell (D_y [μ m]) at the period of 0.33 μ s of the amplitude of ± 15 V. At the non-circle shape of the projected area of the cell, both the length of D_y (the vertical direction) to the flow direction: the electric field direction) and D_x (flow direction) was measured at each cell (Fig. 17b). The shifted distance (Δy) of each cell is compared with that (Δy_0) of the cell with the standard diameter of 18 μ m (D_{y0}), which flows from the similar position (x_0, y_0) at the similar velocity (v_0) with the corresponding cell (Fig. 17c). Fig. 17c shows the relationship between the shifted distance ratio ($\Delta y / \Delta y_0$) and the dimension ratio of the cell (D_y / D_{y0}). The bigger cell tends to make the larger shift.

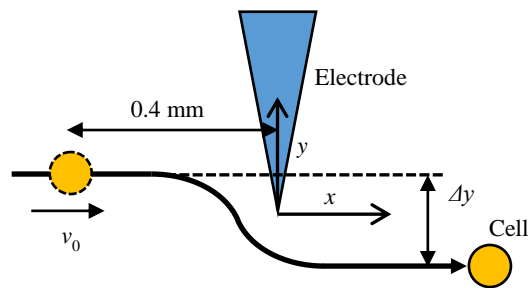


Fig. 9: Movement of cell flowing near tip of electrode.

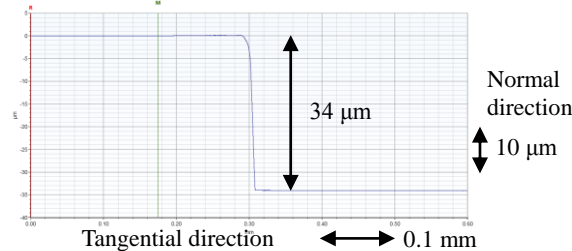


Fig. 10: Tracings of stylus on layer of SU-8 on surface electrode.

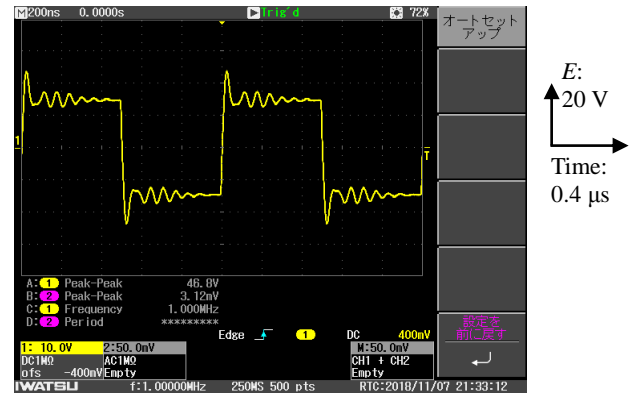


Fig. 11a: Voltage (E) tracings of rectangular wave: period of 1 μ s, amplitude of ± 15 V.

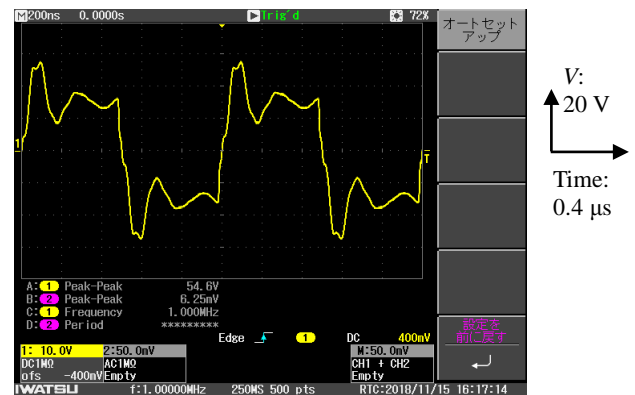


Fig. 11b: Tracings of voltage (V) of rectangular electric stimulation: period of 1 μ s, amplitude of ± 15 V: 7.5 mA (2 kΩ).

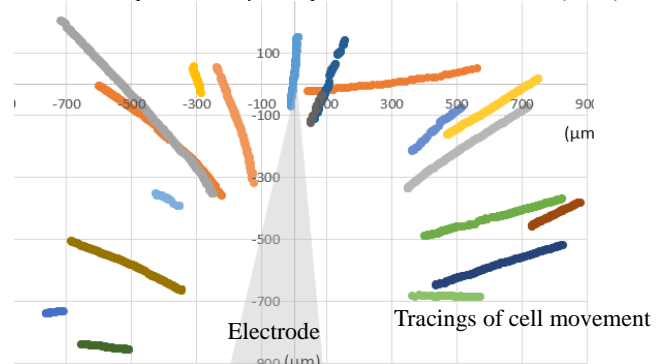


Fig. 12: Tracings of movement of 18 cells in stationary fluid around triangle electrode with rectangular alternating electric stimulation: unit, μ m; period of 1 μ s, amplitude of ± 15 V.

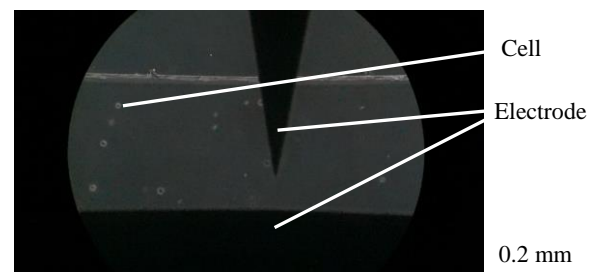


Fig. 13: Cells in flow channel around triangle electrode.

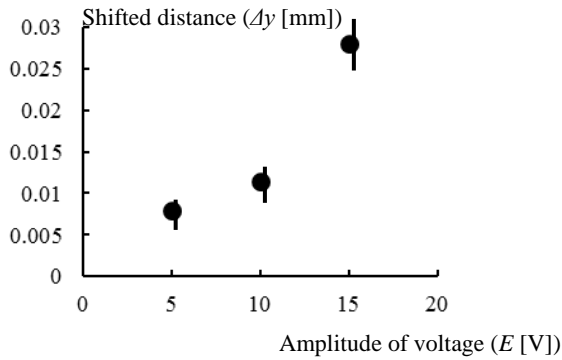


Fig. 14: Relationship between shifted distance (Δy [mm]) and amplitude of voltage (E [V]): mean (circle) \pm standard deviation (bar), $n = 4$.

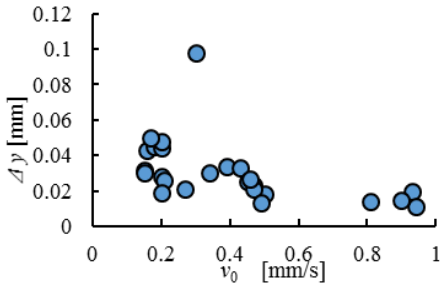


Fig. 15: Relationship between shifted distance (Δy) and initial velocity (v_0). Shift decreases at higher velocity.

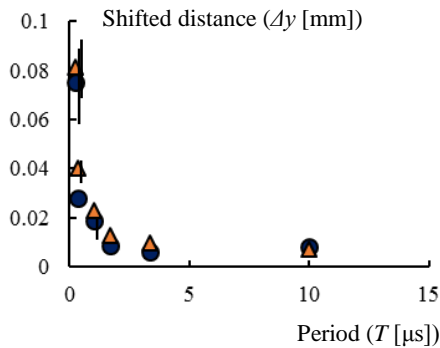


Fig. 16: Relationship between shifted distance (Δy [mm]) and period (T [μs]) of electric stimulation: $0.2 \text{ mm/s} < v_0 < 0.3 \text{ mm/s}$ (triangle), $0.3 \text{ mm/s} < v_0 < 0.4 \text{ mm/s}$ (circle): mean (mark) \pm SD (bar): $n = 4$.

4. DISCUSSION

The dielectrophoresis was applied to the cell sorting system as minimally invasive method in the previous studies [10, 11]. The shift distance has been very small ($< 0.1 \text{ mm}$) in the present experiment. If the shift movement of the cell adjacent to the tip of the electrode is enlarged at the downstream by the inertial movement, the method can be applied to the cell sorting. The relationship between the stream line of the cell and the position of the side wall of the flow channel should be considered for the continuous movement of the cell at the downstream. In another way, the accumulated shift by the multiple electrodes might enlarged the shift movement of the cell. In the present study, the dielectrophoretic movement of the cell was tried to be observed by the optical microscope. The electrodes arrangement with the shorter distance has not been designed, because the electrodes in the present study are not optically

transparent. The shift might depend on the passing route of the cell. The dielectrophoretic effect might be highest adjacent to the tip of the electrode. The shift might depend on the size of the particle [8]. The voltage between electrodes higher than $\pm 15 \text{ V}$ might enlarge the shift. The amplitude of the electric stimulation has been limited within the threshold value to prevent electrolysis [12] in the present study. Figs. 13-17 show the movement of each cell in the x - y plane. The movement of the direction (z) perpendicular to the flow is very small, because the height of the channel is 0.035 mm . The movement of cells between surface electrodes depends on the morphology of surface electrodes (the angle of the tip) [13–16], which relates to non-uniformity of electric field. The higher slope of electric field with non-uniformity is necessary to enlarge the movement of cells around the electrode. In the previous studies, dielectrophoresis has been tried to apply on the biological cell manipulation technology [8–26]. The micro grooves were used for trapping of flowing cells in the previous study [5]. To apply the present system for cell sorting, both the initial position and the velocity should be controlled before the non-uniform electric field in the flow channel.

5. CONCLUSION

A micro flow channel with the surface electrodes has been

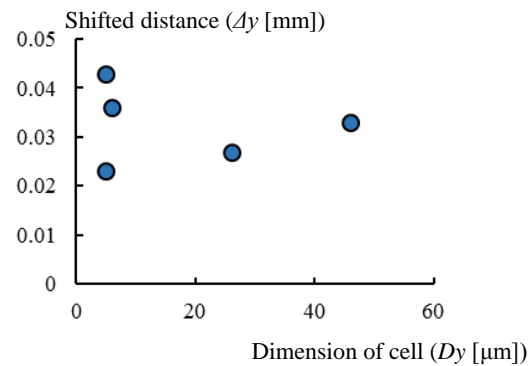


Fig. 17a: Relationship between shifted distance (Δy [mm]) and dimension of cell (D_y [μm]): $0.33 \mu s, \pm 15 \text{ V}$.

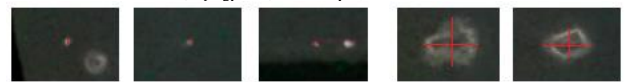


Fig. 17b: Size of cell: D_y (vertical direction, electric field direction) and D_x (flow direction). 50 μm

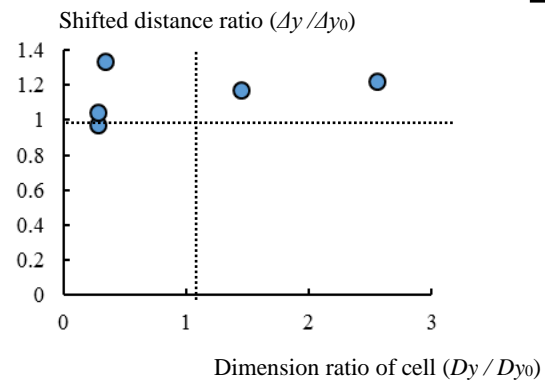


Fig. 17c: Relationship between shifted distance ratio ($\Delta y / \Delta y_0$) and dimension ratio of cell (D_y / D_{y0}).

designed to detect the dielectrophoretic movement of a biological cell *in vitro*. A pair of asymmetric surface electrodes of titanium (thickness of 200 nm) were incorporated in the flow channel by the photolithography technique. The selected system design (the triangular shape of the electrode, electric rectangular alternating current wave (± 7.5 mA, 0.3 μ s of period), and the flow velocity of 0.3 mm/s) is able to detect dielectrophoretic movement of floating C2C12.

REFERENCES

- [1] A. Tabll and H. Ismail, "The Use of Flow Cytometric DNA Ploidy Analysis of Liver Biopsies in Liver Cirrhosis and Hepatocellular Carcinoma", **Journal of World's Largest Science Technology & Medicine**, 2011, pp. 88–107.
- [2] S.M. McFaul, B.K. Lin and H. Ma, "Cell Separation Based on Size and Deformability Using Microfluidic Funnel Ratchets", **Lab on a Chip**, Vol. 12, 2012, pp. 2369–2376.
- [3] Y. Takahashi, S. Hashimoto, H. Hino and T. Azuma, "Design of Slit between Micro Cylindrical Pillars for Cell Sorting", **Journal of Systemics, Cybernetics and Informatics**, Vol. 14, No. 6, 2016, pp. 8–14.
- [4] M. Heijazian, W. Li and N.T. Nguyen, "Lab on a Chip for Continuous-flow Magnetic Cell Separation", **Lab on a Chip**, Vol. 15, No. 4, 2015, pp. 959–970.
- [5] Y. Takahashi, S. Hashimoto, H. Hino, A. Mizoi and N. Noguchi, "Micro Groove for Trapping of Flowing Cell", **Journal of Systemics, Cybernetics and Informatics**, Vol. 13, No. 3, 2015, pp. 1–8.
- [6] H. Imasato and T. Yamakawa, "Measurement of Dielectrophoretic Force by Employing Controllable Gravitational Force", **Journal of Electrophoresis**, Vol. 52, No. 1, 2008, pp. 1–8.
- [7] D.R. Gossett, W.M. Weaver, A.J. Mach, S.C. Hur, H.T.K. Tse, W. Lee, H. Amini and D. DiCarlo, "Label-free Cell Separation and Sorting in Microfluidic Systems", **Analytical and Bioanalytical Chemistry**, Vol. 397, 2010, pp. 3249–3267.
- [8] Y. Kang, D-D. Li, S.A. Kalams and J.E. Eid, "DC-Dielectrophoretic Separation of Biological Cells by Size", **Biomedical Microdevices**, Vol. 10, No. 2, 2008, pp. 243–249.
- [9] H.C. Shim, Y.K. Kwak, C.S. Han and S. Kim, "Effect of a Square Wave on an Assembly of Multi-walled Carbon Nanotubes Using AC Dielectrophoresis", *Physica E*, Vol. 41, 2009, pp. 1137–1142.
- [10] H. Shafiee, J.L. Caldwell, M.B. Sano and R.V. Davalos, "Contactless Dielectrophoresis: a New Technique for Cell Manipulation", **Biomedical Microdevices**, Vol. 11, No. 5, 2009, pp. 997–1006.
- [11] J. Yoshioka, Y. Ohsugi, T. Yoshitomi, T. Yasukawa, N. Sasaki and K. Yoshimoto, "Label-Free Rapid Separation and Enrichment of Bone Marrow-Derived Mesenchymal Stem Cells from a Heterogeneous Cell Mixture Using a Dielectrophoresis Device", **Sensors**, Vol. 18, No. 9, 2018, pp. 1–8.
- [12] G. Mernier, N. Piacentini, T. Braschler, N. Demierre and P. Renaud, "Continuous-flow Electrical Lysis Device with Integrated Control by Dielectrophoretic Cell Sorting", **Lab on a Chip**, Vol. 10, No. 16, 2010, pp. 2077–2082.
- [13] Y. Wakizaka, M. Hakoda and N. Shiragami, "Effect of Electrode Geometry on Dielectrophoretic Separation of Cells", **Biochemical Engineering Journal**, Vol. 20, No. 1, 2004, pp. 13–19.
- [14] B. Yafouz, N.A. Kadri and F. Ibrahim, "Dielectrophoretic Manipulation and Separation of Microparticles Using Microarray Dot Electrodes", **Sensors**, Vol. 14, No. 4, 2014, pp. 6356–6369.
- [15] H. Chu, I. Doh and Y.H. Cho, "A Three-dimensional (3D) Particle Focusing Channel Using the Positive Dielectrophoresis (pDEP) Guided by a Dielectric Structure between Two Planar Electrodes", **Lab on a Chip**, Vol. 9, No. 5, 2009, pp. 686–S691.
- [16] N. Demierre, T. Braschler, P. Linderholm, U. Seger, H. van Lintel and P. Renaud, "Characterization and Optimization of Liquid Electrodes for Lateral Dielectrophoresis", **Lab on a Chip**, Vol. 7, No. 3, 2007, pp. 355–365.
- [17] P.R.C. Gascoyne, X.B. Wang, Y. Huang and F.F. Becker, "Dielectrophoretic Separation of Cancer Cells from Blood", **IEEE Transactions on Industry Applications**, Vol. 33, No. 3, 1997, pp. 670–678.
- [18] S. Fiedler, S.G. Shirley, T. Schnelle, and G. Fuhr, "Dielectrophoretic Sorting of Particles and Cells in a Microsystem", **Analytical Chemistry**, Vol. 70, No. 9, 1998 p. 1909–1915.
- [19] T. Müller, A. Pfennig, P. Klein, G. Gradl, M. Jäger, and T. Schnelle, "The Potential of Dielectrophoresis for Single-Cell Experiments", **IEEE Engineering in Medicine and Biology Magazine**, No. 11/12, 2003, pp. 51–61.
- [20] B.H. Lapizco-Encinas, B.A. Simmons, E.B. Cummings and Y. Fintschenko, "Dielectrophoretic Concentration and Separation of Live and Dead Bacteria in an Array of Insulators", **Analytical Chemistry**, Vol. 76, No. 6, 2004, pp. 1571–1579.
- [21] X. Xuan, B. Xu and D. Li, "Accelerated Particle Electrophoretic Motion and Separation in Converging-diverging Microchannels", **Analytical Chemistry**, Vol. 77, No. 14, 2005, pp. 4323–4328.
- [22] M.D. Vahey and J. Voldman, "An Equilibrium Method for Continuous-Flow Cell Sorting Using Dielectrophoresis", **Analytical Chemistry**, Vol. 80, No. 9, 2008, pp. 3135–3143.
- [23] N. Demierre, T. Braschler, R. Muller and P. Renaud, "Focusing and Continuous Separation of Cells in a Microfluidic Device Using Lateral Dielectrophoresis", **Sensors and Actuators B: Chemical**, Vol. 132, 2008, pp. 388–396.
- [24] J. An, J. Lee, S.H. Lee, J. Park and B. Kim, "Separation of Malignant Human Breast Cancer Epithelial Cells from Healthy Epithelial Cells Using an Advanced Dielectrophoresis-activated Cell Sorter (DACS)", **Analytical and Bioanalytical Chemistry**, Vol. 394, No. 3, 2009, pp. 801–809.
- [25] S. van den Driesche, V. Rao, D. Puchberger-Engel, W. Witariski and M.J. Vellekoop, "Continuous Cell from Cell Separation by Traveling Wave Dielectrophoresis", **Sensors and Actuators B: Chemical**, Vol. 170, 2012, pp. 207–214.
- [26] Y. Takahashi, S. Hashimoto, M. Watanabe and D. Hasegawa, "Dielectrophoretic Movement of Cell around Surface Electrodes in Flow Channel", **Journal of Systemics Cybernetics and Informatics**, Vol. 16, No. 3, 2018, pp. 81–87.
- [27] B.H. Jo, L.M. Van Lerberghe, K.M. Motsegood and D.J. Beebe, "Three-Dimensional Micro-Channel Fabrication in Polydimethylsiloxane (PDMS) Elastomer", **Journal of Microelectromechanical Systems**, Vol. 9, No. 1, 2000, pp. 76–81.

